Differential Quantitative Determination of Site-Specific Intact *N*-glycopeptides in Serum Haptoglobin between Hepatocellular Carcinoma and Cirrhosis using LC-EThcD-MS/MS

*Jianhui Zhu[1], Zhengwei Chen[2], Jie Zhang[1], Mingrui An[1], Jing Wu[1], Qing Yu[3], St John Skilton[4], Marshall Bern[4], K. Ilker Sen[4], Lingjun Li[2,3], and David M. Lubman[1]**

Supporting Information

Table of Contents

Figure S1. SDS-PAGE analysis of the Hp eluent enriched from an HCC serum sample using the antibody-immobilized HPLC column.

Figure S2. Extracted ion chromatograms (XICs) of MS/MS spectra of the HexNAc oxonium ion within the m/z range 204.08-204.09 in early HCC, cirrhosis, and normal controls, respectively.

Figure S3. MS1 spectrum of a low abundant glycopeptide VVLHPN^{241}YSQVD with the glycan A4G4F2S3 showed the isotope distribution, with the S/N ratio greater than 26.

Figure S4. Venn diagrams detail the overlap of (a) site-specific *N*-glycopeptides and (b) glycan compositions of serum haptoglobin among early HCC, cirrhosis, and normal controls.

Figure S5. Heat map of the altered *N*-glycopeptides observed in disease groups (early HCC and cirrhosis) but absent in healthy controls.

Figure S6. The top 10 abundant *N*-glycopeptides normalized against the total *N*-glycopeptides in serum Hp in early HCC, cirrhosis, and normal controls, respectively.

Figure S7. The overall distribution of bi-, tri-, and tetra-antennary *N*-glycoforms on sites N184, N207, and N241 of serum Hp in early HCC, cirrhosis, and normal controls, respectively.

Table S1. The HPLC peak area of the eluted Hp fraction in each serum sample.

Table S2. The list of 279 *N*-glycopeptide spectral matches, including the glycosite, peptide sequence, modification summary, glycan composition, observed *m/z*, *z*, calculated *m/z*, ppm, Byonic score, and retention time.

Table S3. Relative abundance of site-specific intact *N*-glycopeptides identified in serum Hp from early HCC, cirrhosis, and normal controls, respectively.

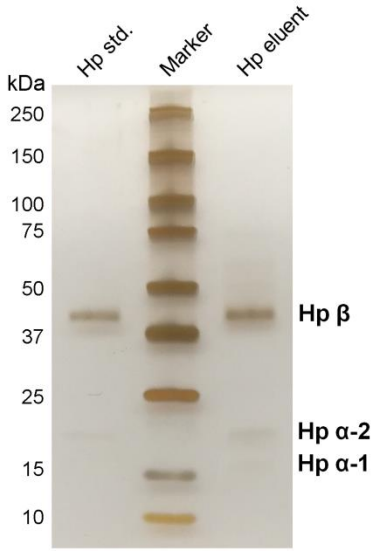

Figure S1. SDS-PAGE analysis of the Hp eluent enriched from an HCC serum sample using the antibody-immobilized HPLC column. One-tenth of Hp eluent was loaded onto the gel, with a comparison of 0.3 μg of a Hp standard. Silver staining result showed the purity of the Hp eluent, including Hp β chain, α-2 chain and α-1 chain. The Hp β chain contains four glycosylation sites.

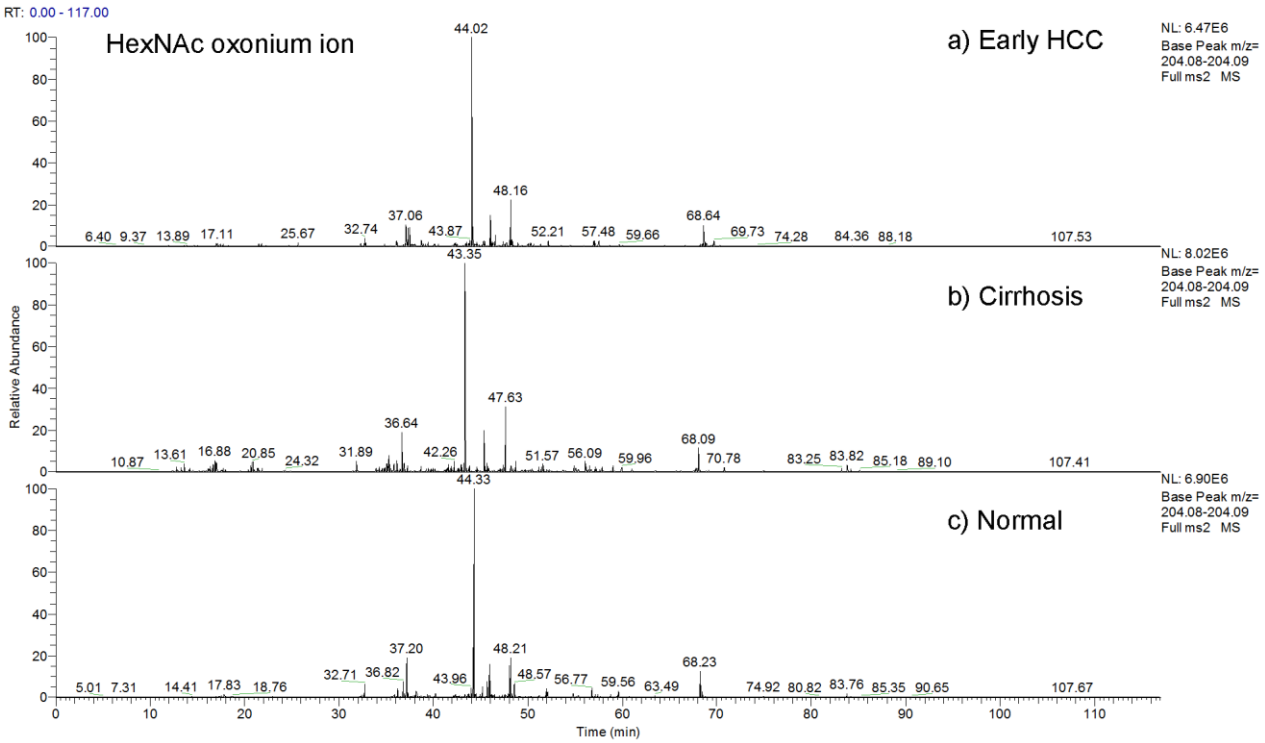

Figure S2. Extracted ion chromatograms (XICs) of MS/MS spectra of the HexNAc oxonium ion within the m/z range 204.08-204.09 in early HCC, cirrhosis, and normal controls, respectively. The major peaks at ~44 min, ~46 min, ~48 min, and ~68 min corresponded to the HexNAc oxonium ion derived from the glycopeptides of VVLHPN^{241}YSQVD, NLFLN^{207}HSE, MVSHHN^{184}LTTGATLINE, and VVLHPN^{241}YSQVDIGLIK, respectively. The small peptide N^{211}ATAK was difficult to detect due to the high hydrophilicity.

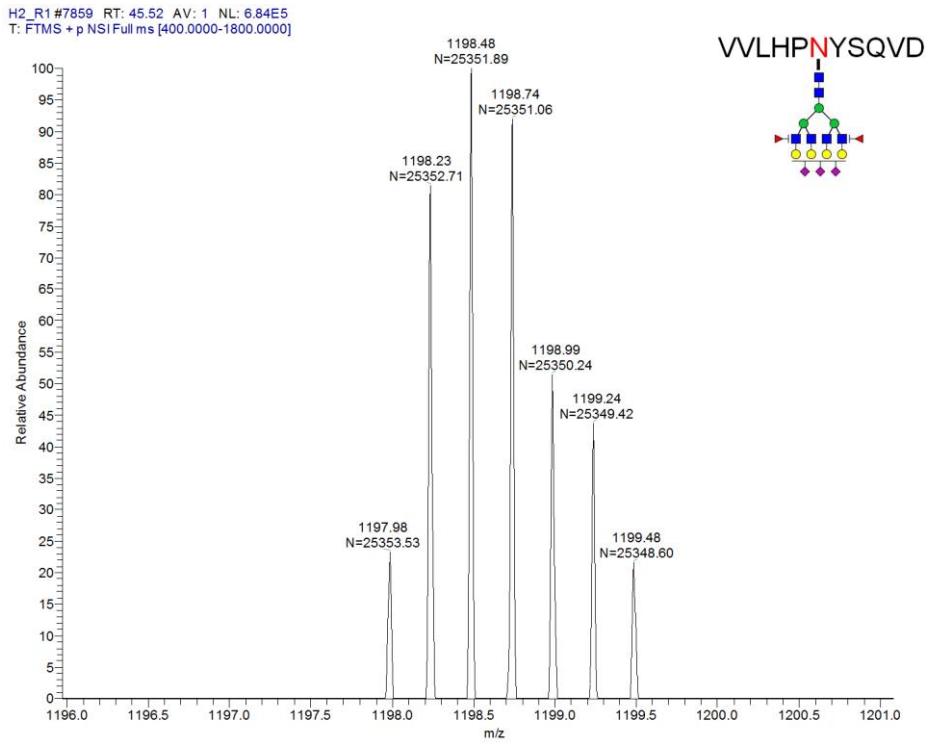

Figure S3. MS1 spectrum of a low abundant glycopeptide VVLHPN^{241}YSQVD with the glycan A4G4F2S3 (m/z=1197.978) showed the isotope distribution. The intensity of the precursor peak was 6.84E5, which was over 26-fold higher than that of noise (the intensity of noise was labeled with 'N=').

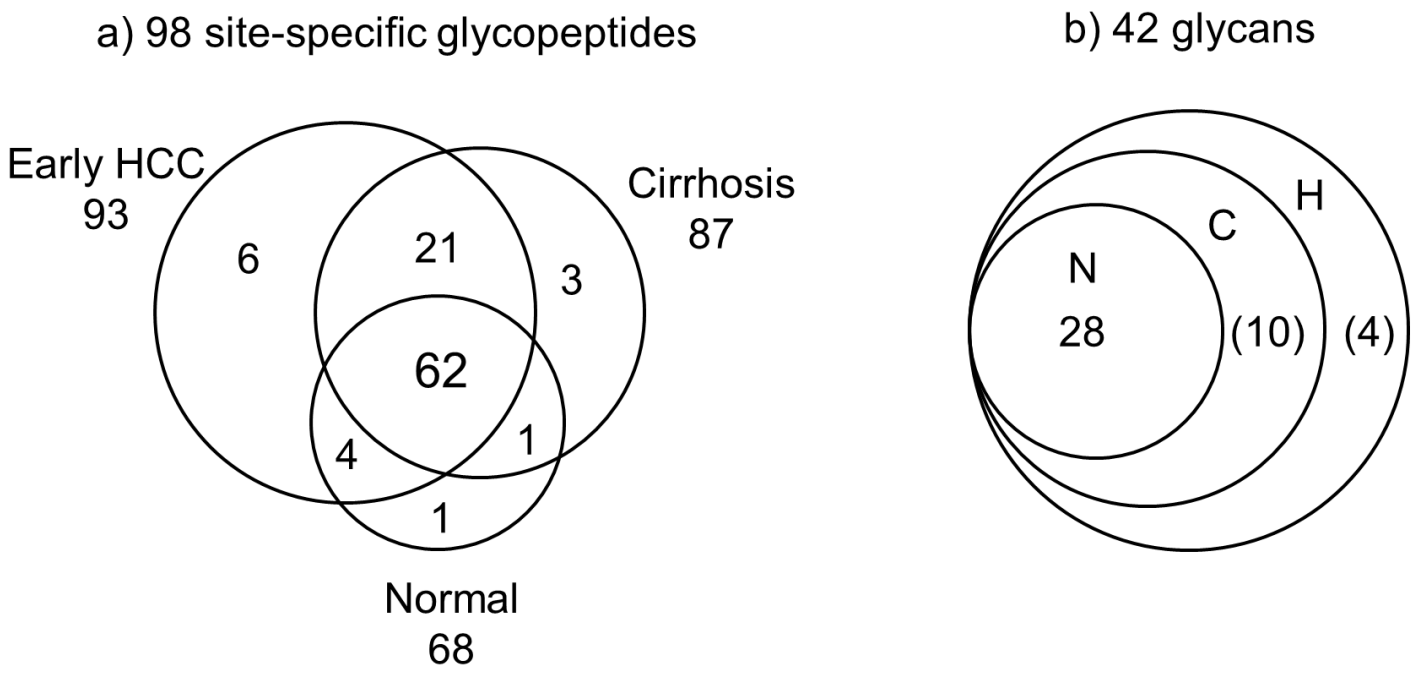

Figure S4. Venn diagrams detail the overlap of (a) site-specific *N*-glycopeptides and (b) glycan compositions of serum haptoglobin among early HCC, cirrhosis, and normal controls. (a) There were 62 intact *N*-glycopeptides commonly identified in all cases, while 21 more site-specific glycopeptides overlapped between early HCC and cirrhosis and 6 site-specific glycopeptides uniquely presented in early HCC. (b) Notably, 4 unique glycan compositions were exclusively identified in early HCC patients but were absent in cirrhosis and normal controls.

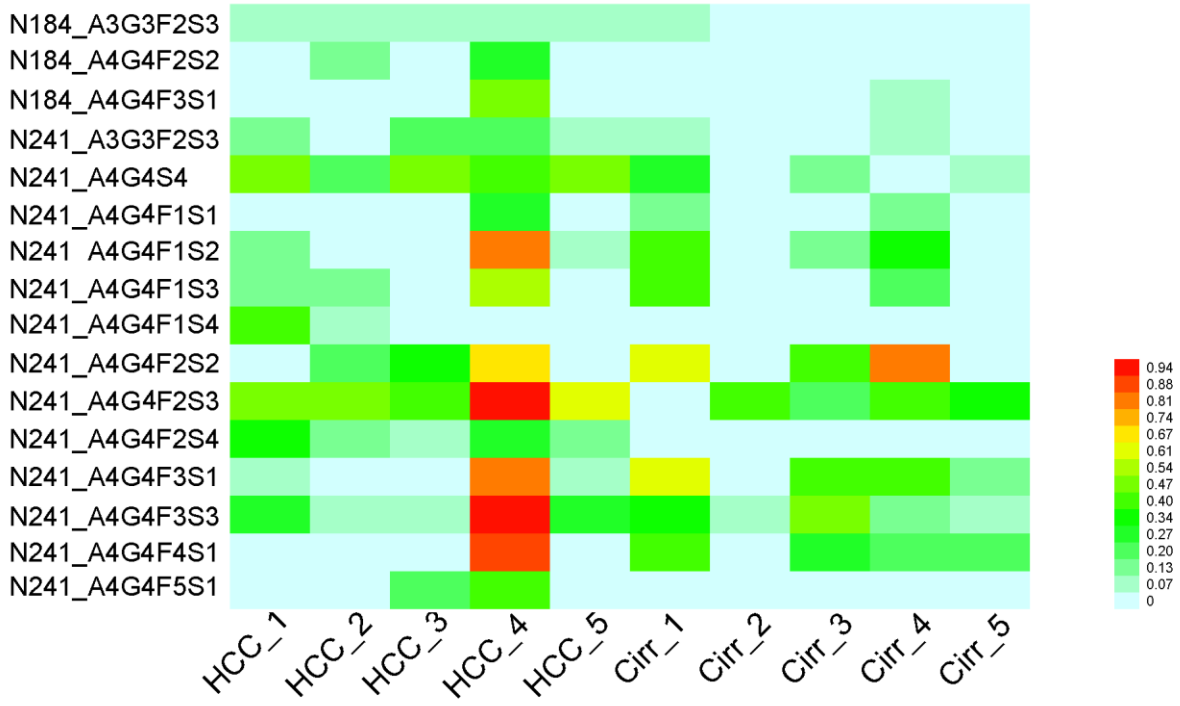

Figure S5. Heat map of the altered *N*-glycopeptides observed in disease groups (5 early HCC and 5 cirrhosis) but absent in healthy controls, which were mainly with tetra-antennary glycans bearing multiple focuses and sialic acids. The heat map was based on the quantitative data of site-specific glycopeptides in each individual patient. HCC represents early HCC patient, and Cirr represents cirrhosis patient. In the case of 5 early HCCs, 43.7% of the altered glycopeptides were identified in all 5 patients, 68.7% in at least 3 patients, and 12.5% in only 1 patient.

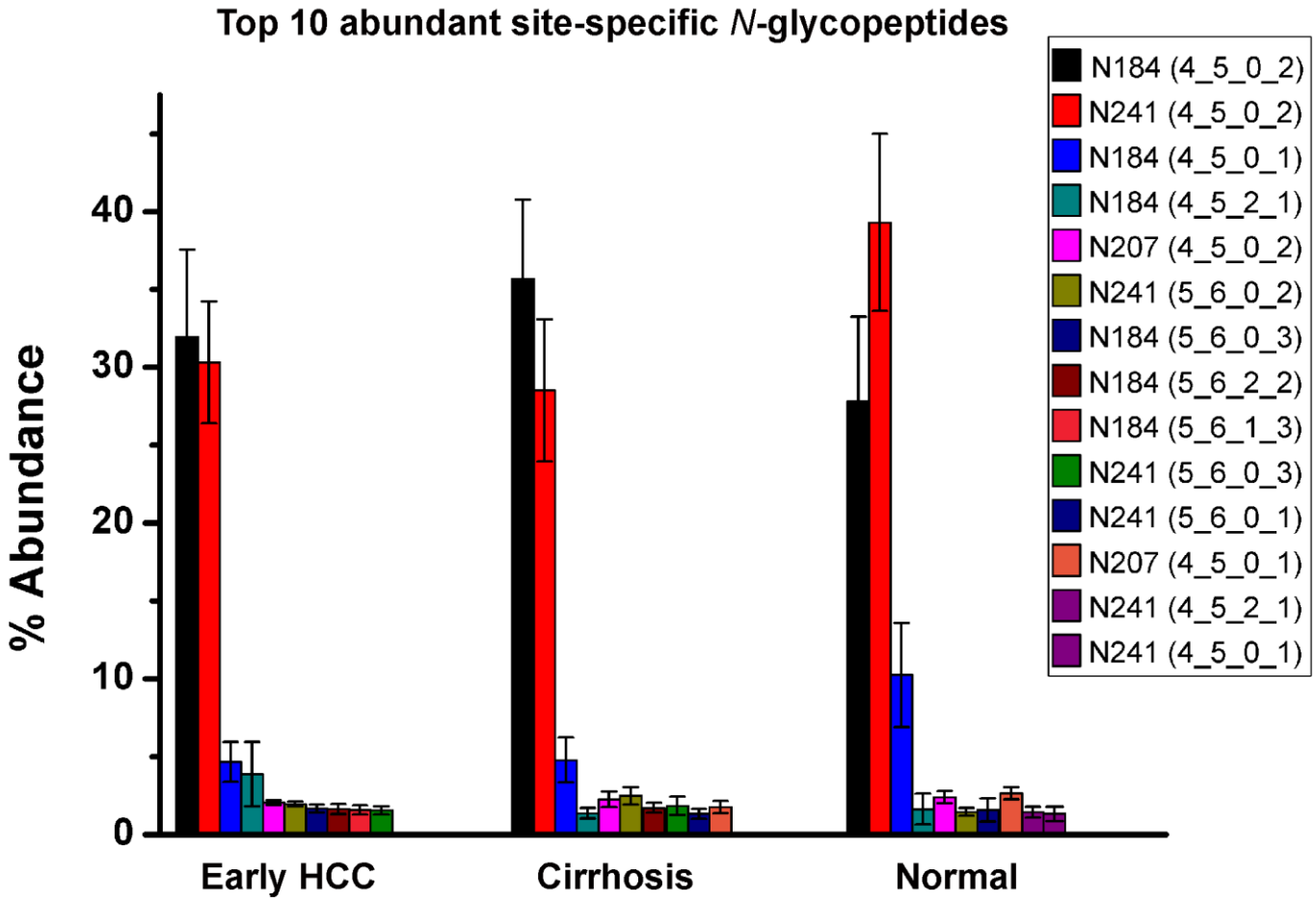

Figure S6. The top 10 abundant *N*-glycopeptides normalized against the total *N*-glycopeptides in serum Hp in early HCC, cirrhosis, and normal controls, respectively. Among the top ten, were predominantly glycopeptides with biantennary glycans, except in the cases of early HCC and cirrhosis where glycopeptides bearing triantennary glycans with one or two fucoses and multiple sialic acids were also included. Overall, the glycopeptides with the biantennary di-sialylated glycan A2G2S2 at N184 and N241 were the two most abundant glycopeptides in all cases, which account for 62.3 ±7.5%, 64.2 ±7.1%, and 67.1 ±6.0% of total *N*-glycopeptides in early HCC, cirrhosis, and normal controls, respectively. The third most abundant glycopeptide was that at site N184 with biantennary monosialylated glycan (A2G2S1), contributing to 4.7 ±1.3%, 4.8 ±1.5%, and 10.2 ±1.2% of total *N*-glycopeptides in the three groups respectively.

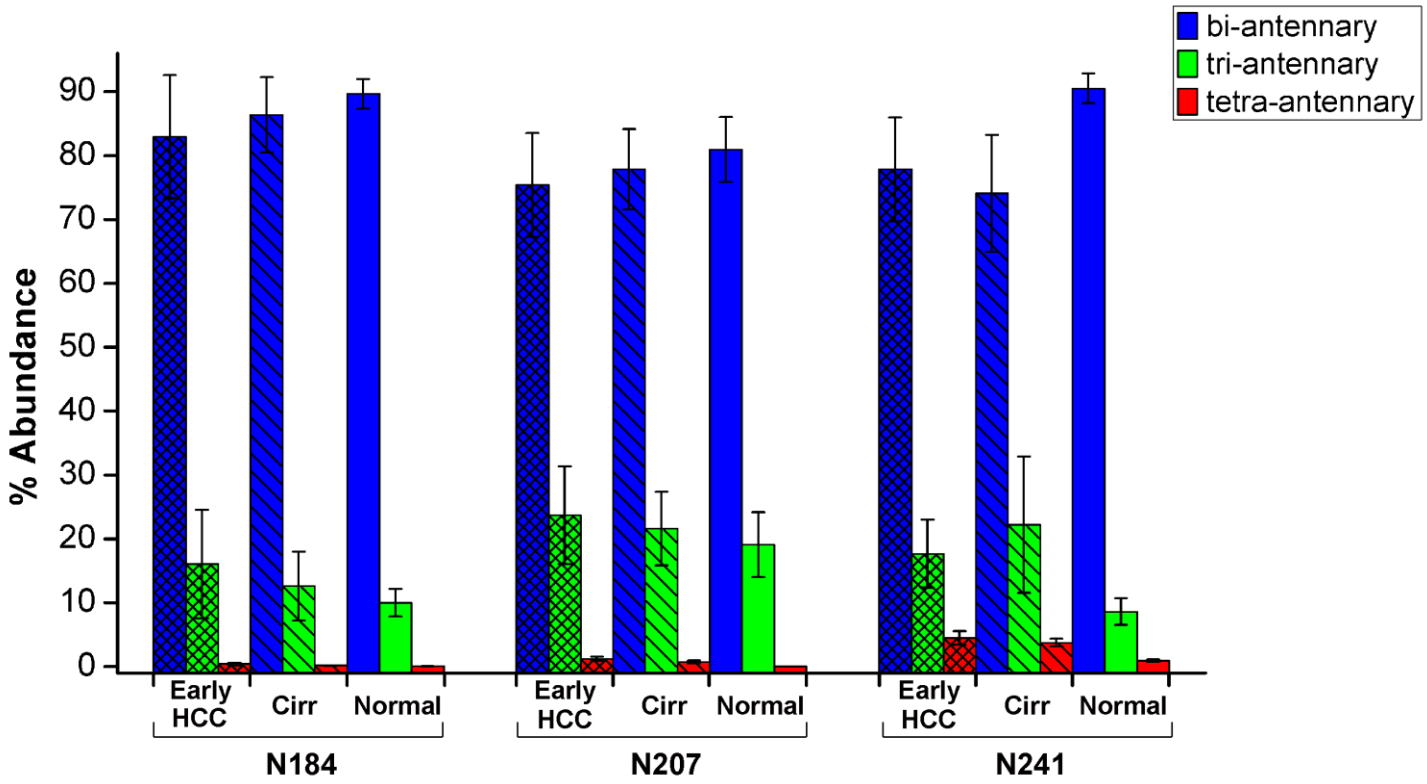

Figure S7. The overall distribution of bi-, tri-, and tetra-antennary *N*-glycoforms on sites N184, N207, and N241 of serum Hp in early HCC, cirrhosis, and normal controls, respectively. In general, the biantennary *N*-glycoforms were the most abundant, which had a >70% contribution in all cases. The triantennary glycoforms were medium abundant, with a 10~28% contribution on the individual sites. The tetra-antennary glycoforms were at low abundance, accounting for 0.05~5% on each site. Notably, the tetraantennary glycoforms were significantly elevated on the site N241 in early HCC and cirrhosis patients compared to normal controls.

Table S1. The HPLC peak area of the eluted Hp fraction in each serum sample.

	Hp Peak area		Hp Peak area		Hp peak area
Early HCC1	2,619,374	Cirrhosis1	3,403,647	Normal1	2,356,369
Early HCC2	2,754,842	Cirrhosis2	2,499,394	Normal2	2,356,508
Early HCC3	2,490,231	Cirrhosis3	3,535,080	Normal3	2,248,255
Early HCC4	2,365,822	Cirrhosis4	4,118,733	Normal4	2,294,872
Early HCC5	2,094,719	Cirrhosis5	3,682,093	Normal5	3,237,703

Table S3. Relative abundance of site-specific intact *N*-glycopeptides identified in serum Hp from early HCC, cirrhosis, and normal controls, respectively. The mean value of relative abundance of glycopeptide at each site is listed where the abundance of a glycopeptide was normalized against the sum of all glycopeptides at the same glycosite. A 4-digit nomenclature was employed for the annotation of glycan composition in an order of HexNAc_Hex_Fuc_NeuAc (HexNAc=N-acetylhexosamine; Hex=Hexose; Fuc=Fucose; NeuAc=sialic acid).

Site	Glycopeptide (Peptide seq.[a] + Glycan composition)	*m/z*	*z*[b]	Early HCC, %		Cirrhosis, %		Normal, %	
				mean	range	mean	range	mean	range
N184	MVSHH**N**^{184}LTTGATLINE + 3_4_0_1	1096.139	3+	0.732	0.643-1.430	1.088	1.07-2.07	1.004	0.526-1.81
	MVSHH**N**^{184}LTTGATLINE + 4_4_0_1	1163.833	3+	0.013	0-0.131	ND[c]	n/a[d]	0.068	0.054-0.119
	MVSHH**N**^{184}LTTGATLINE + 4_5_0_0	1120.818	3+	0.128	0.076-0.379	0.181	0-0.527	0.471	0.389-0.574
	MVSHH**N**^{184}LTTGATLINE + 4_5_0_1	913.639	4+	9.410	4.38-11.70	9.558	7.57-14.20	22.16	18.2-24.0
	MVSHH**N**^{184}LTTGATLINE + 4_5_0_2	986.413	4+	61.59	59.10-77.70	69.65	57.80-84.60	60.82	51.60-67.30
	MVSHH**N**^{184}LTTGATLINE + 4_5_1_1	950.154	4+	1.223	0.282-3.17	1.465	0.226-4.21	0.391	0.142-0.692
	MVSHH**N**^{184}LTTGATLINE + 4_5_1_2	1022.928	4+	2.561	0.672-3.84	2.066	1.50-5.61	1.546	0.498-0.954
	MVSHH**N**^{184}LTTGATLINE + 4_5_2_1	986.668	4+	7.271	2.791-8.90	2.339	0-6.71	3.192	0-6.70
	MVSHH**N**^{184}LTTGATLINE + 4_6_0_1	954.153	4+	0.314	0-0.821	0.839	0.312-0.927	0.279	0.086-0.626
	MVSHH**N**^{184}LTTGATLINE + 5_4_0_2	996.667	4+	0.330	0-1.06	0.112	0-0.442	0.245	0-0.60
	MVSHH**N**^{184}LTTGATLINE + 5_5_0_2	1037.183	4+	0.008	0-0.084	0.006	0-0.061	ND	n/a
	MVSHH**N**^{184}LTTGATLINE + 5_5_1_1	1000.924	4+	0.356	0.074-1.91	0.226	0-0.902	0.488	0.137-0.696
	MVSHH**N**^{184}LTTGATLINE + 5_6_0_1	1004.923	4+	0.539	0.16-1.40	0.412	0.088-0.636	0.548	0.293-0.716
	MVSHH**N**^{184}LTTGATLINE + 5_6_0_2	1077.696	4+	1.176	0.95-2.65	1.506	1.22-2.07	1.325	1.02-2.13
	MVSHH**N**^{184}LTTGATLINE + 5_6_0_3	1150.470	4+	3.346	3.11-4.79	1.529	0.589-2.66	3.516	2.14-4.17
	MVSHH**N**^{184}LTTGATLINE + 5_6_1_1	1041.437	4+	0.100	0-0.564	0.084	0-0.193	0.004	0-0.036
	MVSHH**N**^{184}LTTGATLINE + 5_6_1_2	1114.211	4+	1.070	0.672-2.45	1.139	0.583-3.41	0.066	0-0.0369
	MVSHH**N**^{184}LTTGATLINE + 5_6_1_3	1186.985	4+	3.354	1.61-6.61	2.215	1.73-3.57	0.642	0.242-1.16

	MVSHH**N**^{184}LTTGATLINE +	5_6_2_1	1077.951	4+	0.612	0.227-1.51	0.328	0.097-0.968	0.640	0.371-1.18
	MVSHH**N**^{184}LTTGATLINE +	5_6_2_2	1150.725	4+	3.426	2.10-5.38	3.353	3.12-5.03	2.417	1.01-3.67
	MVSHH**N**^{184}LTTGATLINE +	5_6_2_3	1223.499	4+	0.106	0.09-0.129	0.033	0-0.083	ND	n/a
	MVSHH**N**^{184}LTTGATLINE +	5_6_3_1	1114.466	4+	0.809	0-2.61	0.874	0.0175-1.48	0.115	0-0.404
	MVSHH**N**^{184}LTTGATLINE +	5_6_4_1	1150.980	4+	0.832	0-2.06	0.774	0-1.41	ND	n/a
	MVSHH**N**^{184}LTTGATLINE +	6_7_0_1	1096.206	4+	0.020	0.017-0.0927	0.010	0-0.069	ND	n/a
	MVSHH**N**^{184}LTTGATLINE +	6_7_0_2	1168.979	4+	0.080	0.032-0.189	0.038	0-0.14	0.013	0-0.066
	MVSHH**N**^{184}LTTGATLINE +	6_7_0_3	1241.753	4+	0.021	0.016-0.077	0.015	0-0.082	0.017	0-0.054
	MVSHH**N**^{184}LTTGATLINE +	6_7_1_1	1132.720	4+	0.018	0-0.181	0.021	0-0.0627	ND	n/a
	MVSHH**N**^{184}LTTGATLINE +	6_7_1_2	1205.494	4+	0.005	0-0.0483	0.006	0-0.0586	ND	n/a
	MVSHH**N**^{184}LTTGATLINE +	6_7_1_3	1278.268	4+	0.002	0-0.198	ND	n/a	ND	n/a
	MVSHH**N**^{184}LTTGATLINE +	6_7_2_1	1169.235	4+	0.040	0-0.278	0.014	0-0.139	0.006	0-0.050
	MVSHH**N**^{184}LTTGATLINE +	6_7_2_2	1242.008	4+	0.066	0-0.297	0.013	0-0.013	ND	n/a
	MVSHH**N**^{184}LTTGATLINE +	6_7_3_1	1205.749	4+	0.106	0-0.486	0.036	0-0.082	ND	n/a
	MVSHH**N**^{184}LTTGATLINE +	6_7_4_1	1242.263	4+	0.026	0-0.261	ND	n/a	ND	n/a
	MVSHH**N**^{184}LTTGATLINE +	7_8_0_1	1187.489	4+	0.317	0.156-1.90	0.075	0-0.445	0.029	0-0.145
N207	NLFL**N**^{207}HSE +	3_4_0_0	1115.965	2+	1.842	0-5.29	4.409	1.816-10.70	1.860	0.894-2.95
	NLFL**N**^{207}HSE +	3_4_0_1	1261.513	2+	0.434	0-1.02	0.480	0.756-1.09	0.703	0.741-1.02
	NLFL**N**^{207}HSE +	4_5_0_0	1298.531	2+	0.050	0-0.502	0.100	0-0.618	0.447	0.286-1.01
	NLFL**N**^{207}HSE +	4_5_0_1	963.055	3+	27.66	25.90-32.50	28.36	29.50-38.50	40.33	35.80-43.70
	NLFL**N**^{207}HSE +	4_5_0_2	1060.087	3+	39.69	31.0-51.90	38.74	26.90-44.80	36.10	30.70-45.50
	NLFL**N**^{207}HSE +	4_5_1_1	1011.741	3+	4.659	2.67-10.50	4.751	2.11-8.34	1.042	0-2.89
	NLFL**N**^{207}HSE +	4_5_1_2	1108.773	3+	1.911	1.75-4.03	0.990	0.61-2.53	0.472	0-1.38
	NLFL**N**^{207}HSE +	4_6_0_1	1017.073	3+	0.013	0-2.02	ND	n/a	0.069	0-0.137
	NLFL**N**^{207}HSE +	5_6_0_1	1084.766	3+	4.322	2.89-4.38	4.567	3.85-5.09	3.405	2.29-4.12
	NLFL**N**^{207}HSE +	5_6_0_2	1181.798	3+	6.088	3.22-	6.056	3.46-	8.818	5.43-

					15.10		7.41		14.50
	NLFL**N**^{207}HSE + 5_6_0_3	959.374	4+	4.864	2.70-6.20	3.813	2.69-6.41	4.513	0.994-6.17
	NLFL**N**^{207}HSE + 5_6_1_1	1133.452	3+	1.359	0.809-3.37	1.157	1.10-2.85	0.307	0.116-0.843
	NLFL**N**^{207}HSE + 5_6_1_2	1230.484	3+	3.348	2.03-6.37	3.808	3.34-4.69	1.111	0.36-1.66
	NLFL**N**^{207}HSE + 5_6_1_3	1327.515	3+	2.245	1.48-3.15	1.584	0.702-3.52	0.305	0-1.28
	NLFL**N**^{207}HSE + 5_6_2_1	1182.138	3+	ND	n/a	0.132	0-0.625	0.418	0-2.105
	NLFL**N**^{207}HSE + 5_6_2_2	959.629	4+	0.505	0-0.656	ND	n/a	0.104	0-0.51
	NLFL**N**^{207}HSE + 5_6_3_1	1230.824	3+	ND	n/a	0.313	0-1.25	ND	n/a
	NLFL**N**^{207}HSE + 6_7_0_1	1206.477	3+	0.257	0.20-0.907	0.042	0-0.209	ND	n/a
	NLFL**N**^{207}HSE + 6_7_0_2	977.883	4+	0.093	0-0.925	0.102	0.067-0.625	ND	n/a
	NLFL**N**^{207}HSE + 6_7_1_1	1255.163	3+	0.136	0-0.625	0.144	0-0.937	ND	n/a
	NLFL**N**^{207}HSE + 6_7_1_2	1014.398	4+	ND	n/a	0.119	0-0.705	ND	n/a
	NLFL**N**^{207}HSE + 6_7_3_1	1014.653	4+	0.524	0-1.38	0.335	0-0.89	ND	n/a
N211	**N**^{211}ATAK + 4_5_0_2	903.688	3+	ND	n/a	ND	n/a	58.16	0-100
	N^{211}ATAK + 5_6_0_3	1122.431	3+	53.43	0-40.60	ND	n/a	36.65	0-87.40
	N^{211}ATAK + 5_6_1_3	1171.117	3+	16.37	0-31.50	ND	n/a	ND	n/a
	N^{211}ATAK + 5_6_2_2	1122.771	3+	30.20	0-100	100	0-100	5.190	0-19.30
N241	VVLHP**N**^{241}YSQVD + 3_4_0_0	1264.550	2+	0.047	0-0.154	0.106	0.063-0.17	0.050	0-0.062
	VVLHP**N**^{241}YSQVD + 3_4_0_1	940.401	3+	1.134	0.803-1.77	1.496	1.13-2.08	1.342	1.26-1.60
	VVLHP**N**^{241}YSQVD + 4_4_0_1	1008.094	3+	0.008	0-0.078	0.036	0-0.168	0.051	0-0.0826
	VVLHP**N**^{241}YSQVD + 4_5_0_1	1062.111	3+	2.002	1.76-3.08	3.226	2.30-5.19	2.843	2.14-3.31
	VVLHP**N**^{241}YSQVD + 4_5_0_2	1159.143	3+	69.42	61.5-76.7	65.65	57.80-75.80	82.76	79.50-84.70
	VVLHP**N**^{241}YSQVD + 4_5_1_1	1110.797	3+	0.217	0.105-0.797	0.430	0.255-1.40	0.071	0-0.164
	VVLHP**N**^{241}YSQVD + 4_5_1_2	906.124	4+	1.211	0.479-3.28	1.251	0.447-2.22	0.601	0.169-2.15
	VVLHP**N**^{241}YSQVDIGLIK + 4_5_2_1	1000.957	4+	3.645	1.03-10.40	1.555	0-1.85	2.624	0-7.49
	VVLHP**N**^{241}YSQVD + 4_6_0_1	1116.129	3+	0.157	0-0.542	0.307	0.21-0.76	0.166	0.119-0.333
	VVLHP**N**^{241}YSqVDIGLIK + 5_4_0_2	1011.204	4+	ND	n/a	0.014	0-0.136	ND	n/a

VVLHP**N**[241]YSQVD +	5_5_1_1	1178.491	3+	0.049	0-0.168	0.147	0.163-0.282	0.111	0-0.198
VVLHP**N**[241]YSQVD +	5_6_0_1	1183.822	3+	1.705	0.661-2.46	3.111	1.94-5.21	1.390	1.06-1.47
VVLHP**N**[241]YSQVD +	5_6_0_2	960.892	4+	4.422	2.35-5.99	5.851	3.48-7.99	3.092	2.05-3.97
VVLHP**N**[241]YSQVD +	5_6_0_3	1033.666	4+	3.554	2.61-6.25	4.155	2.80-4.76	2.707	1.02-3.68
VVLHP**N**[241]YSQVD +	5_6_1_1	1232.508	3+	0.494	0.066-1.86	0.827	0.066-2.21	0.016	0-0.0329
VVLHP**N**[241]YSQVD +	5_6_1_2	1329.540	3+	0.813	0.255-3.01	1.290	0.298-2.24	0.040	0.023-0.093
VVLHP**N**[241]YSQVD +	5_6_1_3	1070.181	4+	2.017	0.708-3.24	2.290	0.972-3.75	0.415	0.133-0.747
VVLHP**N**[241]YSQVD +	5_6_2_1	1281.194	3+	1.305	0.404-4.46	1.468	0.109-5.14	0.301	0-0.773
VVLHP**N**[241]YSQVD +	5_6_2_2	1033.921	4+	1.751	1.20-3.16	1.893	1.55-2.68	0.493	0-1.33
VVLHP**N**[241]YSQVD +	5_6_2_3	1106.695	4+	0.133	0.102-0.212	0.032	0-0.085	ND	n/a
VVLHP**N**[241]YSQVDIGLIK +	5_6_3_1	1128.754	4+	0.192	0.161-1.42	0.105	0-0.596	0.022	0-0.079
VVLHP**N**[241]YSQVD +	5_6_4_1	1034.176	4+	1.239	1.30-2.67	1.003	0.873-1.69	ND	n/a
VVLHP**N**[241]YSQVD +	6_7_0_1	979.402	4+	0.148	0.049-0.279	0.233	0.087-0.397	0.061	0.032-0.191
VVLHP**N**[241]YSQVD +	6_7_0_2	1052.175	4+	0.599	0.343-1.58	0.558	0.506-1.02	0.277	0.127-0.561
VVLHP**N**[241]YSQVD +	6_7_0_3	1124.949	4+	0.557	0.482-0.953	0.526	0.497-1.05	0.318	0.227-0.545
VVLHP**N**[241]YSQVD +	6_7_0_4	1197.723	4+	0.438	0.24-0.527	0.130	0-0.316	0.164	0.103-0.38
VVLHP**N**[241]YSQVD +	6_7_1_1	1015.916	4+	0.057	0-0.283	0.079	0-0.18	ND	n/a
VVLHP**N**[241]YSQVD +	6_7_1_2	1088.690	4+	0.210	0.142-0.82	0.192	0-0.409	ND	n/a
VVLHP**N**[241]YSQVD +	6_7_1_3	1161.464	4+	0.190	0.093-0.281	0.134	0-0.401	ND	n/a
VVLHP**N**[241]YSQVD +	6_7_1_4	1234.238	4+	0.089	0.052-0.442	ND	n/a	ND	n/a
VVLHP**N**[241]YSQVD +	6_7_2_1	1052.430	4+	0.178	0.102-0.744	0.378	0.319-0.709	0.076	0-0.132
VVLHP**N**[241]YSQVD +	6_7_2_2	1125.204	4+	0.272	0-0.699	0.409	0-0.859	ND	n/a

	VVLHP**N**[241]YSQVD +	6_7_2_3	1197.978	4+	0.615	0.413-1.007	0.299	0-0.409	0.014	0-0.055
	VVLHP**N**[241]YSQVD +	6_7_2_4	1270.752	4+	0.217	0.091-0.351	ND	n/a	ND	n/a
	VVLHP**N**[241]YSQVD +	6_7_3_1	1088.945	4+	0.247	0.065-0.874	0.326	0-0.61	ND	n/a
	VVLHP**N**[241]YSQVD +	6_7_3_3	1234.493	4+	0.354	0.085-1.005	0.244	0.082-0.49	ND	n/a
	VVLHP**N**[241]YSQVD +	6_7_4_1	1125.459	4+	0.182	0-0.912	0.244	0-0.460	ND	n/a
	VVLHP**N**[241]YSQVD +	6_7_5_1	1161.974	4+	0.136	0-0.465	ND	n/a	ND	n/a

[a] Most common peptide sequences for each glycoform are listed.

[b] The charge represents the most abundant charge state of each glycopeptide.

[c] ND, not detected.

[d] n/a, not applicable.